Proceedings of the
44th IEEE Conference on Decision and Control, and
the European Control Conference 2005
Seville, Spain, December 12-15, 2005

A multicriteria image-based controller based on a mixed polytopic and norm-bounded representation of uncertainties

Sophie Tarbouriech, Philippe Souères, Bo Gao

***Abstract*— This paper presents a multicriteria image-based controller to position a 3-DOF camera with respect to a target. The proposed controller allows to stabilize the camera and determine the associated region of stability in spite of unknown value of the target points depth, bounds on admissible visual feature errors which guarantee visibility, and limits on the camera velocity and acceleration. The description of the closed-loop system is based on a mixed polytopic and norm-bounded representation of uncertainties combined with an original sector condition. This formulation allows to consider LMI-based optimization schemes for computing the feedback gain that leads to the maximization of the size of the region of stability associated to the closed-loop system. Simulations of the control method are presented in the case of a camera mounted on a pan-platform supported by a cart-like robot.**

***Index Terms*— Visual servoing, image-base control, saturation control, visibility, constraint satisfaction.**

I. Introduction

Visual servoing techniques aim at using the information provided by one or several cameras to control the motion of robotics systems. Since the early methods [6], very much has been done to increase the robustness of controllers and tackle the potential problem of stability and convergence underlined in [2]. The robustness issues mainly concern the design of stable controllers despite parametric uncertainties and the guarantee of target visibility. Several approaches have been proposed in the frame of image-based [3], pose-based [18], [15], [19], or hybrid [8] methods.

In this paper, we consider that the error is directly expressed in terms of 2D visual features, and the depth of the target points is bounded but unknown. In [7], a 2D vision-based controller, robust to image distortion and camera orientation, was proposed to servo a planar manipulator. To enlarge the region of stability of the controller, which is usually limited by local minima, a potential switching strategy was proposed in [5]. In the case that the initial and desired robot's position are distant, the combination of image-based control with path planning in the image was proposed in [11] to increase the control robustness. In [10], the robustness of 2D visual servoing with respect to image processing errors was addressed by using statistical techniques. Robust stability and the guarantee of no attractive local minima have also been obtained by considering extended-2D coordinates which include information on the depth distribution of points and the estimated camera model [13]. As shown in [9], the uncertainty in the depth distribution of target points strongly reduces the domain of stability of the system. In most part of methods, the robustness improvement comes from the introduction of geometric arguments which allow to complete the local information in the image. Though the geometric reasoning turns out to be essential in this problem, the judicious choice of the controller is also fundamental to guarantee the satisfaction of constraints. However, in a large part of works, the control design is not considered as the major issue. Following the formalism introduced in [3], the closed-loop controller is deduced from the regulation of a task function. and the stabilization of the system is often obtained by imposing the exponential decay of this task function.

The authors are with LAAS-CNRS, 7 Avenue du Colonel Roche, 31077 Toulouse cedex 4, France. tarbour@laas.fr, soueres@laas.fr, bgao@laas.fr

In order to derive a better benefit from advanced control techniques, a general framework was proposed in [17] to model image-based control problems with constraints. The approach was based on the combination of both robust quadratic methods and saturation nonlinearities representation via the use of differential inclusion results. The main drawback of this approach was that the conditions were given in the form of bilinear matrix inequalities (BMIs). In [14] a LPV approach was proposed to synthesize a robust active vision system. A general framework for synthesis and analysis of multicriteria vision-based servocontrol schemes was also proposed in [1]. This approach was based on a rational state-space representation of the system, embedded in Structured Normed Linear Differential Inclusion. In this paper we present an example of application of advanced control techniques to the design of a multicriteria image-based controller. The problem is stated in the framework of the task function approach. The proposed controller allows to stabilize a 3-DOF camera in front of a target, and determine the associated region of stability in spite of unknown value of the target points depth, bounds on admissible feature errors which guarantee visibility, and limits on the camera velocity and acceleration. We consider a description of the closed-loop system based on both polytopic and norm-bounded uncertainties combined with an original sector condition. Hence, the provided conditions are directly in an LMI form for given bounds on admissible image feature error. Such a formulation allows to consider LMI-based optimization schemes for computing the feedback gain that lead to the maximization of the size of the region of stability associated to the closed-loop system.

The problem statement is presented in section II and the control synthesis is described in section III. Simulations of the control method are presented in section IV for the case of a camera mounted on a pan-platform supported by a cart-like robot.

Notations. For any vector $x \in \Re^n$, $x \succeq 0$ means that all the components of x, denoted $x_{(i)}$, are nonnegative. For two vectors $x,\ y\ \in\ \Re^n$, the notation $x \succeq y$ means that $x_{(i)} - y_{(i)} \geq 0$, $\forall i = 1, \ldots, n$. The elements of a matrix $A \in \Re^{m\times n}$ are denoted by $A_{(i,l)}$, $i = 1, \ldots, m$, $l = 1, \ldots, n$. $A_{(i)}$ denotes the ith row of matrix A. For two symmetric matrices, A and B, $A > B$ means that $A - B$ is positive definite. A' denotes the transpose of A. $D(x)$ denotes a diagonal matrix obtained from vector x. 1_m denotes the m-order vector $1_m = [1 \ldots 1]' \in \Re^m$. I_m denotes the m-order identity matrix. $Co\{.\}$ denotes a convex hull. For $u \in \Re^m$, $sat_{u_0}(u_{(i)}) = sign(u_{(i)}) \min(|u_{(i)}|, u_{0(i)})$ with $u_{0(i)} > 0$, $i = 1, ..., m$.

II. Problem Statement

We consider the problem of positioning a 3-DOF camera with respect to a visual target. The camera is supposed to be supported by a robotic system which allows any horizontal translations and rotations about the vertical axis. An application to the case of a camera mounted on a pan-platform supported by a wheeled robot will be considered in section IV. The objective of the paper is to design a stabilizing controller and determine the associated region of stability in spite of the following constraints:

- **C1**: The depth of the target points with respect to the camera frame, is bounded but unknown.
- **C2**: The visual signal errors, in the image, must remain bounded during the stabilization process to ensure visibility.
- **C3**: the velocity and the acceleration of the camera must remain bounded to satisfy the limits on the actuator dynamics.

In return, we will make the hypothesis that the intrinsic parameters of the camera are known and consider the metric pinhole model with focal length $f = 1$.

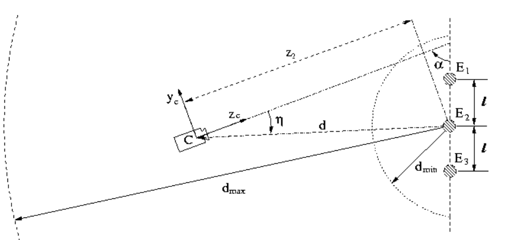

Fig. 1. Description of parameters for the vision-based task

Let R be an absolute frame attached to the scene and R_c a frame attached to the camera, having its origin at the optical center C and its z-axis directed along the optical axis. Let $T \in \Re^3$ denote the reduced kinematic screw of the camera which expresses the translational and rotational velocities of R_C with respect to R, expressed in R_C. As the motion is restricted to the horizontal plane, a linear target of three equidistant points E_i, $i = 1, 2, 3$, located at the same height as C, allows to perform the positioning task. We will denote by $l > 0$ the distance between the target points, α the angle between the target line and the optical axis, and η the angle between the optical axis and the line (CE_2) (see Fig. 1). The camera is initially located in the left half-plane delimited by the target line and the distance $d = CE_2$ is bounded as follows:

$$d \in [d_{min}, d_{max}] \tag{1}$$

Furthermore, to prevent from projection singularities, the following condition is considered:

$$\alpha \in [-\pi + \alpha_{min}, -\alpha_{min}] \tag{2}$$

where $\alpha_{min} > 0$ is a small angle. For $i = 1, 2, 3$, let us denote respectively by Y_i and Y_i^* the ordinates of the current and desired target points in the image plane. Following the formalism introduced in [3], [12], a simple choice for the positioning task function is: $e = [\ e_1 \quad e_2 \quad e_3\ ]' \in \Re^3$ with $e_i = Y_i - Y_i^*$. The desired camera position corresponds to: $Y_2^* = 0$ and $Y_3^* = -Y_1^*$. In addition, to guarantee the visibility of the target, we impose the following bound on task function components:

$$|e_i| \leq \beta,\ i = 1, 2, 3\ ;\ \text{with } \beta > 0 \tag{3}$$

Consequently, the angle η is bounded by:

$$|\eta| \leq \eta_{max} = \arctan(\beta) < \pi/2 \tag{4}$$

and therefore, the depth $z_2 = d\cos(\eta)$ of the central point E_2 is bounded as follows:

$$z_2 \in [d_{min}\cos(\eta_{max}), d_{max}] \tag{5}$$

The relation between the time-derivative of the task function and the kinematic screw is given by the optical flow equations:

$$\dot{e} = L(z, e)T \tag{6}$$

where the image Jacobian $L(z, e) \in \Re^{3\times 3}$ is defined by:

$$L(z,e) = \begin{bmatrix} -1/z_1 & (e_1 + Y_1^\star)/z_1 & 1 + (e_1 + Y_1^\star)^2 \\ -1/z_2 & (e_2 + Y_2^\star)/z_2 & 1 + (e_2 + Y_2^\star)^2 \\ -1/z_3 & (e_3 + Y_3^\star)/z_3 & 1 + (e_3 + Y_3^\star)^2 \end{bmatrix} \tag{7}$$

In (6) and (7), the constraints on the vector $z = [\ z_1 \quad z_2 \quad z_3\ ]' \in \Re^3$ follow the description given in Fig.1. From relations (1), (2), (4) and (5), the depth of target points E_1 and E_3 can be expressed in terms of the depth z_2 of the central point E_2. Hence, it follows

$$z = [z_2 + l cos(\alpha),\ z_2,\ z_2 - l cos(\alpha)]'$$

As $l << z_2$ the following approximation can be done:

$$\begin{array}{l} \frac{1}{z_1} \simeq \frac{1}{z_2}(1 - \frac{l\cos(\alpha)}{z_2}) = \frac{1}{z_2} - \frac{l\cos(\alpha)}{z_2^2} = p_1 - p_2 \\ \frac{1}{z_2} = p_1 \\ \frac{1}{z_3} \simeq \frac{1}{z_2}(1 + \frac{l\cos(\alpha)}{z_2}) = \frac{1}{z_2} + \frac{l\cos(\alpha)}{z_2^2} = p_1 + p_2 \end{array} \tag{8}$$

From the definition of the admissible intervals relative to z_2 and α given by (2) and (5), it follows that the scalars p_1 and p_2 in (8) satisfy $p_{jmin} \leq p_j \leq p_{jmax}$, $j = 1, 2$. Thus, matrix $L(z, e)$ depends on two uncertain parameters p_1 and p_2. In order to take into account the limits on the actuators dynamics the following bounds on the kinematics screw and its time-derivative will be considered:

$$-u_1 \preceq T \preceq u_1 \quad (9)$$
$$-u_0 \preceq \dot{T} \preceq u_0 \quad (10)$$

To solve objectives C1, C2, C3 previously defined, the following extended state vector is defined:

$$\xi = \begin{bmatrix} e \\ T \end{bmatrix} \in \Re^6 \quad (11)$$

with the following matrices

$$\mathbb{A}(z,\xi) = \begin{bmatrix} 0 & L(z,e) \\ 0 & 0 \end{bmatrix} \in \Re^{6\times 6}$$
$$\mathbb{B} = \begin{bmatrix} 0 \\ I_3 \end{bmatrix} \in \Re^{6\times 3} \quad (12)$$

Thus, we consider the following system

$$\dot{\xi} = \mathbb{A}(z,\xi)\xi + \mathbb{B}\dot{T} \quad (13)$$

where the acceleration of the camera $\dot{T}$ is the control vector. Hence, in order to take into account the constraint (10), the control law under consideration has the following form:

$$\dot{T} = sat_{u_0}(\mathbb{K}\xi) \text{ with } \mathbb{K} = [\ K_1 \quad K_2\ ] \in \Re^{3\times 6} \quad (14)$$

Hence, the closed-loop system reads:

$$\dot{\xi} = \mathbb{A}(z,\xi)\xi + \mathbb{B}sat_{u_0}(\mathbb{K}\xi) \quad (15)$$

Relative to (15), one has to take into account the constraints (3) and (9), which means that the state ξ must belong to the following polyhedral set $\Omega(\xi)$:

$$\Omega(\xi) = \{\xi \in \Re^6; -\begin{bmatrix} \beta 1_3 \\ u_1 \end{bmatrix} \preceq \xi \preceq \begin{bmatrix} \beta 1_3 \\ u_1 \end{bmatrix}\} \quad (16)$$

The problem we intend to solve throughout the paper with respect to the closed-loop system (15), subject to constraints (16), can be summarized as follows.

Problem 1: Determine a gain $\mathbb{K}$ and a region of stability, as large as possible, such that

- the asymptotic stability of the closed-loop system (15) is guaranteed in spite of uncertainties on the depth of the target points with respect to the camera frame.
- the boundedness on the visual signal errors and the velocity are satisfied.

III. Control Synthesis

A. Preliminary Results

The closed-loop system (15) can be also described by:

$$\dot{\xi} = (\mathbb{A}(z,\xi) + \mathbb{B}\mathbb{K})\xi + \mathbb{B}\phi(\mathbb{K}\xi) \quad (17)$$

with the decentralized dead-zone nonlinearity $\phi(\mathbb{K}\xi) = sat_{u_0}(\mathbb{K}\xi) - \mathbb{K}\xi$, defined by: $\forall i = 1,2,3$,

$$\phi(\mathbb{K}_{(i)}\xi) = \begin{cases} u_{0(i)} - \mathbb{K}_{(i)}\xi & \text{if } \mathbb{K}_{(i)}\xi > u_{0(i)} \\ 0 & \text{if } |\mathbb{K}_{(i)}\xi| \le u_{0(i)} \\ -u_{0(i)} - \mathbb{K}_{(i)}\xi & \text{if } \mathbb{K}_{(i)}\xi < -u_{0(i)} \end{cases} \quad (18)$$

As in the formalism developed in [4], consider a matrix $\mathbb{G} \in \Re^{3\times 6}$ and define the following set:

$$S(u_0) = \{\xi \in \Re^6; -u_0 \preceq (\mathbb{K} - \mathbb{G})\xi \preceq u_0\} \quad (19)$$

The following lemma can then be stated.

Lemma 2: [4] Consider the nonlinearity $\phi(\mathbb{K}\xi)$ defined in (18). If $\xi \in S(u_0)$ then the relation:

$$\phi(\mathbb{K}\xi)' M(\phi(\mathbb{K}\xi) + \mathbb{G}\xi) \le 0 \quad (20)$$

is satisfied for any diagonal positive definite matrix $M \in \Re^{3\times 3}$.

B. Main Results

Let us first define the following matrices

$$\mathbb{R} = [\ I_3 \quad 0\ ]; \mathbb{C} = [\ 0 \quad I_3\ ] \quad (21)$$

In order to solve our control design problem, we propose to pursue the strategy summarized as follows.

Theorem 3: If there exist a positive definite function $V(\xi)$ ($V(\xi) > 0$, $\forall \xi \neq 0$), a gain $\mathbb{K}$, a matrix $\mathbb{G}$ and a positive scalar γ satisfying, for any admissible z:

$$\begin{array}{l} \frac{\partial V}{\partial \xi}[(\mathbb{A}(z,\xi) + \mathbb{B}\mathbb{K})\xi + \mathbb{B}\phi(\mathbb{K}\xi)] \\ -2\phi(\mathbb{K}\xi)' M(\phi(\mathbb{K}\xi) + \mathbb{G}\xi) < 0 \end{array} \quad (22)$$

$$\gamma V(\xi) - \xi'(\mathbb{K}_{(i)} - \mathbb{G}_{(i)})' \frac{1}{u_{0(i)}^2}(\mathbb{K}_{(i)} - \mathbb{G}_{(i)})\xi \ge 0,\ i = 1,2,3 \quad (23)$$

$$\gamma V(\xi) - \xi' \mathbb{R}'_{(i)} \frac{1}{\beta^2} \mathbb{R}_{(i)}\xi \ge 0,\ i = 1,2,3 \quad (24)$$

$$\gamma V(\xi) - \xi' \mathbb{C}'_{(i)} \frac{1}{u_{1(i)}^2} \mathbb{C}_{(i)}\xi \ge 0,\ i = 1,2,3 \quad (25)$$

then the gain $\mathbb{K}$ and the set $S(V,\gamma) = \{\xi \in \Re^6; V(\xi) \le \gamma^{-1}\}$ are solutions to Problem 1.

Proof. The satisfaction of relation (23) means that the set $S(V,\gamma)$ is included in the set $S(u_0)$ defined as in (19). Thus, one can conclude that for any $\xi \in S(V,\gamma)$ the nonlinearity $\phi(\mathbb{K}\xi)$ satisfies the sector condition (20). Moreover, the satisfaction of relations (24) and (25) means that the set $S(V,\gamma)$ is included in the set $\Omega(\xi)$ defined by (16). Thus, for any $\xi \in S(V,\gamma)$, the constraints C2 and C3 are respected. Consider a positive definite function $V(\xi)$ ($V(\xi) > 0$, $\forall \xi \neq 0$). We want to prove that the time-derivative of V is strictly negative along the trajectories of the closed-loop system (17) for all admissible nonlinearity $\phi(\mathbb{K}\xi)$ and all admissible uncertain vector z. Hence, by using Lemma 2, one gets:

$$\dot{V}(\xi) \le \dot{V}(\xi) - 2\phi(\mathbb{K}\xi)' M(\phi(\mathbb{K}\xi) + \mathbb{G}\xi)$$

Thus, the satisfaction of relation (22) implies that

$$\dot{V}(\xi) - 2\phi(\mathbb{K}\xi)' M(\phi(\mathbb{K}\xi) + \mathbb{G}\xi) < 0$$

therefore $\dot{V}(\xi) < 0$ along the trajectories of system (17). Since this reasoning is valid for any $\xi \neq 0$ belonging to $S(V,\gamma)$, one can conclude that $S(V,\gamma)$ is a set of stability for the saturated closed-loop system. □

Theorem 3 provides a sufficient condition to solve the control gain design. However, such a condition is not really constructive to exhibit a suitable function $V(\xi)$, a gain $\mathbb{K}$ and a scalar γ. The idea then consists in considering a quadratic function for $V(\xi)$, as $V(\xi) = \xi' P \xi$, $P = P' > 0$.

Furthermore, we have also to write in a tractable way the matrix $\mathbb{A}(z, \xi)$, and therefore the closed-loop system (17). In this sense, by defining the following matrices:

$$B_1(z) = \begin{bmatrix} -1/z_1 & Y_1^*/z_1 & 1 + (Y_1^*)^2 \\ -1/z_2 & Y_2^*/z_2 & 1 + (Y_2^*)^2 \\ -1/z_3 & Y_3^*/z_3 & 1 + (Y_3^*)^2 \end{bmatrix};$$

$$B_2(z) = \begin{bmatrix} 1/z_1 & 0 & 0 \\ 0 & 1/z_2 & 0 \\ 0 & 0 & 1/z_3 \end{bmatrix};$$

$$D(e) = \begin{bmatrix} e_1 & 0 & 0 \\ 0 & e_2 & 0 \\ 0 & 0 & e_3 \end{bmatrix}; B_3 = \begin{bmatrix} 2Y_1^* & 0 & 0 \\ 0 & 2Y_2^* & 0 \\ 0 & 0 & 2Y_3^* \end{bmatrix}$$

the closed-loop system reads:

$$\begin{aligned} \dot{\xi} = \; & (\mathbb{R}' B_1(z) \mathbb{C} + \mathbb{R}' T_{(2)} B_2(z) \mathbb{R} \\ & + \mathbb{R}' T_{(3)} (B_3 + D(e)) \mathbb{R} + \mathbb{B}\mathbb{K}) \xi + \mathbb{B} \phi(\mathbb{K}\xi) \end{aligned} \quad (26)$$

Thus, from (8), $B_1(z)$ and $B_2(z)$ depend on two uncertain parameters p_1 and p_2. It follows that $B_1(z)$ and $B_2(z)$ belong to a polytope with 4 vertices given by the combinations of value of p_1 and p_2 in their definition interval:

$$\begin{aligned} B_1(z) & \in Co\{B_{1j}, j = 1, ..., 4\} \\ B_2(z) & \in Co\{B_{2j}, j = 1, ..., 4\} \end{aligned} \quad (27)$$

The following proposition derived from Theorem 3 can then be stated.

Proposition 4: If there exist symmetric positive definite matrices $W \in \Re^{6 \times 6}$, $R_1 \in \Re^{3 \times 3}$, a diagonal positive matrix $S \in \Re^{3 \times 3}$, two matrices $Y \in \Re^{3 \times 6}$ and $Z \in \Re^{3 \times 3}$, two positive scalars ϵ and γ satisfying[1]:

$$\begin{bmatrix} \begin{array}{c} W\mathbb{A}_{1j}' + \mathbb{A}_{1j} W + \mathbb{B} Y + Y' \mathbb{B}' \\ + \mathbb{R}'(R_1 + \epsilon u_{1(3)}^2 (1 + \beta^2) I_3) \mathbb{R} \end{array} & \star & \star & \star \\ u_{1(2)} B_{2j} \mathbb{R} W & -R_1 & \star & \star \\ \begin{bmatrix} B_3 \\ I_3 \end{bmatrix} \mathbb{R} W & 0 & -\epsilon I_6 & \star \\ S\mathbb{B}' - Z & 0 & 0 & -2S \end{bmatrix} < 0 \quad (28)$$

$$\begin{bmatrix} W & \star \\ Y_{(i)} - Z_{(i)} & \gamma u_{0(i)}^2 \end{bmatrix} \geq 0, \; i = 1, 2, 3 \quad (29)$$

$$\begin{bmatrix} W & \star \\ \mathbb{R}_{(i)} W & \gamma \beta^2 \end{bmatrix} \geq 0, \; \forall i = 1, 2, 3 \quad (30)$$

$$\begin{bmatrix} W & \star \\ \mathbb{C}_{(i)} W & \gamma u_{1(i)}^2 \end{bmatrix} \geq 0, \; \forall i = 1, 2, 3 \quad (31)$$

then the gain matrix $\mathbb{K} = Y W^{-1}$ and the set

$$\mathcal{E}(W, \gamma) = \left\{ \xi \in \Re^6; \xi' W^{-1} \xi \leq \gamma^{-1} \right\} \quad (32)$$

[1] $\star$ stands for symmetric blocks.

solve Problem 1.

Proof. The proof mimics the one of Theorem 3. The satisfaction of relation (29) means that the set $\mathcal{E}(W, \gamma)$ defined in (32) is included in the set $S(u_0)$ defined in (19). Thus, one can conclude that for any $\xi \in \mathcal{E}(W, \gamma)$ the nonlinearity $\phi(\mathbb{K}\xi)$ satisfies the sector condition (20) with $\mathbb{G} = Z W^{-1}$. Furthermore, the satisfaction of relations (30) and (31) implies that the set $\mathcal{E}(W, \gamma)$ is included in the sets $\Omega(\xi)$ defined in (16). Hence, for any admissible uncertain vector z (see equation (27)) and any admissible vector belonging to $\mathcal{E}(W, \gamma)$, the closed-loop system (17) or (26) can be written as:

$$\begin{aligned} \dot{\xi} \; = \; & (\sum_{j=1}^{4} \lambda_j (\mathbb{A}_{1j} + \mathbb{R}' T_{(2)} B_{2j} \mathbb{R}) \\ & + \mathbb{R}' T_{(3)} (B_3 + D(e)) \mathbb{R} + \mathbb{B}\mathbb{K}) \xi + \mathbb{B} \phi(\mathbb{K}\xi) \end{aligned} \quad (33)$$

with

$$\sum_{j=1}^{4} \lambda_j = 1, \lambda_j \geq 0 \text{ , and } \mathbb{A}_{1j} = \mathbb{R}' B_{1j} \mathbb{C} = \begin{bmatrix} 0 & B_{1j} \\ 0 & 0 \end{bmatrix}$$

The time-derivative of $V(\xi) = \xi' W^{-1} \xi$ along the trajectories of system (33) writes:

$$\begin{aligned} \dot{V}(\xi) \; \leq \; & 2\xi' W^{-1} (\sum_{j=1}^{4} \lambda_j (\mathbb{A}_{1j} + \mathbb{R}' T_{(2)} B_{2j} \mathbb{R}) \\ & + \mathbb{R}' T_{(3)} (B_3 + D(e)) \mathbb{R} + \mathbb{B} Y W^{-1}) \xi \\ & + 2\xi' W^{-1} \mathbb{B} \phi(\mathbb{K}\xi) \\ & - 2\phi(\mathbb{K}\xi)' M (\phi(\mathbb{K}\xi) + Z W^{-1} \xi) \end{aligned}$$

By convexity one can prove that the right term of the above inequality is negative definite if one verifies:

$$\begin{aligned} & 2\xi' W^{-1} (\mathbb{A}_{1j} + \mathbb{R}' T_{(2)} B_{2j} \mathbb{R} + \mathbb{R}' (B_3 + D(e)) \mathbb{R} \\ & + \mathbb{B} Y W^{-1}) \xi + 2\xi' W^{-1} \mathbb{B} \phi(\mathbb{K}\xi) \\ & - 2\phi(\mathbb{K}\xi)' M (\phi(\mathbb{K}\xi) + Z W^{-1} \xi) < 0 \end{aligned}$$

Thus, by using (9) one can upper-bound the term containing $T_{(2)}$ as follows

$$\begin{aligned} 2\xi' W^{-1} \mathbb{R}' T_{(2)} B_{2j} \mathbb{R} \xi \; \leq \; & \xi' (W^{-1} \mathbb{R}' R_1 \mathbb{R} W^{-1} \\ & + u_{1(2)}^2 \mathbb{R}' B_{2j}' R_1^{-1} B_{2j} \mathbb{R}) \xi \end{aligned}$$

with $R_1 = R_1' > 0$. By the same way by using both (9) and (16), one can upper-bound the term containing $T_{(3)}$ and $D(e)$ as follows

$$\begin{aligned} 2\xi' W^{-1} \mathbb{R}' T_{(3)} (B_3 + D(e)) \mathbb{R} \xi \leq \xi' (\epsilon u_{1(3)}^2 (1 + \beta^2) \mathbb{R}' \mathbb{R} \\ + \epsilon^{-1} \mathbb{R}' \begin{bmatrix} B_3' & I_3 \end{bmatrix} \begin{bmatrix} B_3 \\ I_3 \end{bmatrix} \mathbb{R}) \xi \end{aligned}$$

the satisfaction of relation (28) with $M = S^{-1}$ and $\mathbb{K} = Y W^{-1}$, $\mathbb{G} = Z S^{-1}$ allows to verify that $\dot{V}(\xi) < 0$ along the trajectories of system (33). Hence, one can conclude that for any $\xi \in \mathcal{E}(W, \gamma)$, $\xi \neq 0$, $\dot{V}(\xi) < 0$ along the trajectories of system (17). Therefore the set $\mathcal{E}(W, \gamma)$ is a set of asymptotic stability for system (17). □

It is possible to add some conditions about the speed of convergence of the Lyapunov function: for example, one can search for verifying $\dot{V}(\xi)+2\lambda V(\xi)<0$, $\lambda>0$. In this case, it suffices to add the term $2\lambda W$ in the matrix block (1,1) in (28).

C. Optimization Issues

Based on the results of the previous section, we present some convex optimization problem in order to obtain a state feedback gain matrix that ensures the local stability of the closed-loop system (17). It is important to note that relations (28), (29), (30) and (31) of Proposition 4 are LMIs. Furthermore, we aim to design the state feedback gain in order to maximize the estimate of the basin of attraction associated to it (respecting all the constraints on e and T). In other words, we want to compute $\mathbb{K}$ such that the associated region of asymptotic stability is as large as possible considering some size criterion. Thus, the following convex optimization problem can be considered:

$$\begin{array}{c} \min_{W,R_1,Y,Z,S,\gamma,\epsilon} \gamma+\delta+\sigma \\ \text{subject to} \\ \text{relations } (28),(29),(30),(31), \\ \begin{bmatrix} \sigma I_6 & \star \\ Y & I_3 \end{bmatrix} \geq 0, \begin{bmatrix} \delta I_6 & \star \\ I_6 & W \end{bmatrix} \geq 0 \end{array} \tag{34}$$

The last two constraints are added to guarantee a satisfactory conditioning number for matrices $\mathbb{K}$ and W.

D. Possible Extension

The study of system (15) subject to constraints (16) means that the constraints on the error (C2) and on the velocity (part 1 of C3) are linearly respected (saturation avoidance case). On the contrary, saturation of the acceleration (part 2 of C3) is allowed. Nevertheless, if one wants to consider that saturation on the velocity is also allowed then one can modify the closed-loop system as follows:

$$\begin{array}{rcl} \dot{e} & = & L(z,e)sat_{u_1}(u) \\ \dot{u} & = & sat_{u_0}(K_1 e + K_2 sat_{u_1}(u)) \\ T & = & sat_{u_1}(u) \end{array} \tag{35}$$

Thus, by considering $\xi_n = [\ e' \quad u'\ ]' \in \Re^6$ and the same type of matrices than in (12), the closed-loop system reads:

$$\begin{array}{rcl} \dot{\xi}_n & = & (\mathbb{A}(z,\xi_n)+\mathbb{B}\mathbb{K})\xi_n + \mathbb{B}\phi_0 \\ & & +(\begin{bmatrix} L(z,e) \\ 0 \end{bmatrix} + \mathbb{B}K_2)\phi_1 \end{array} \tag{36}$$

where $\phi_0 = sat_{u_0}(K_1 e + K_2 sat_{u_1}(u)) - (K_1 e + K_2 sat_{u_1}(u)) = sat_{u_0}(\mathbb{K}\xi_n + K_2\phi_1) - (\mathbb{K}\xi_n + K_2\phi_1)$ and $\phi_1 = sat_{u_1}(u) - u = sat_{u_1}(\mathbb{C}\xi_n) - \mathbb{C}\xi_n$. In this case, Problem 1 will be studied with respect to system (36) by using nested deadzone nonlinearities as in [16].

IV. Application

In this section we present a result of simulation of the proposed control scheme in the case that the camera is mounted on a pan-platform supported by a wheeled robot. As described in Fig. 2, x and y are the coordinates of the robot reference point M with respect to $R(O,X,Y,Z)$, θ is the direction of the vehicle with respect to the X-axis, and θ_p is the direction of the pan-platform with respect to the robot's main direction. A frame $R_P(P,X_P,Y_P,Z_P)$ is attached to the pan-platform whose origin is at the center of rotation P. The transformation between R_P and R_C consists of an horizontal translation of vector $[\ a \quad b \quad 0\ ]'$ and a rotation of angle $\frac{\pi}{2}$ about the Y_P-axis. Dx is the distance between M and P. The velocities of the robot, which

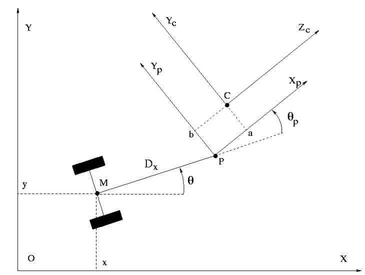

Fig. 2. Camera fixed on a pan-platform supported by a wheeled robot

constitutes the actual system inputs are described by the vector $\dot{q} = [\ v \quad \omega \quad \omega_p\ ]'$, where v and ω are the linear and the angular velocities of the cart with respect to R, while ω_p is the pan-platform angular velocity with respect to R_M. We consider the following kinematic model:

$$\begin{bmatrix} \dot{x} \\ \dot{y} \\ \dot{\theta} \\ \dot{\theta}_p \end{bmatrix} = \begin{bmatrix} \cos(\theta) & 0 & 0 \\ \sin(\theta) & 0 & 0 \\ 0 & 1 & 0 \\ 0 & 0 & 1 \end{bmatrix} \begin{bmatrix} v \\ \omega \\ \omega_p \end{bmatrix}$$

The kinematic screw T is linked to the velocity vector by the relation $T = J(q)\dot{q}$, in which the robot Jacobian is given by:

$$J(q) = \begin{bmatrix} -\sin(\theta_p) & D_x\cos(\theta_p)+a & a \\ \cos(\theta_p) & D_x\sin(\theta_p)-b & -b \\ 0 & -1 & -1 \end{bmatrix} \tag{37}$$

As the proposed method allows to guarantee the stability of the closed-loop system despite unknown value of the target point depth, the simulation has been done by taking the expression of the interaction matrix $L(z^*,e)$ at the final position. With respect to the absolute frame R, the coordinates of the target points are: $E_1(10m, 0.5m)$, $E_2(10m, 0m)$ and $E_3(10m, -0.5m)$. The interval of distance between the robot and camera is $d \in [2.454m, 8m]$. At the expected position, the visual features are defined by: $Y_1^* = 0.2$, $Y_2^* = 0$, and $Y_3^* = -0.2$. To guarantee the visibility we considered $\beta = 0.4$. The initial robot's configuration is given by: $x = 4.85m$, $y = -1m$, $\theta_0 = 0rad$ and $\theta_p = 0.175rad$, and the initial value of the state vector is: $\xi(0) = [-0.0825m; 0.0229m; 0.125m; 0ms^{-1}; 0ms^{-1}; 0rad^{-1}]$. The bounds on the camera velocity and acceleration are $u_1 = [1\ 1\ 0.1]'$, and $u_0 = [1\ 1\ 5]'$. By applying the proposed control scheme with the Matlab LMI Control Toolbox we obtained the following value for the control gain $\mathbb{K}$:

$$\mathbb{K} = \begin{bmatrix} -152.8 & 465.5 & -153.8 & -7.7 & 0.4 & 13.4 \\ -191.2 & 34.8 & 161 & 0 & -10 & 0.4 \\ -1290.8 & -1115.5 & -1364.4 & 66.9 & -3.7 & -350.2 \end{bmatrix}$$

Fig. 3 represents the robot trajectory and the visual features evolution. Though the camera positioning task is perfectly performed, the trajectory is less direct than what is usually obtained by imposing the exponential decay of the task function. The velocities of the robot and the kinematic screw of the camera are described in Fig. 4. As shown, the kinematic screw remains within the prescribed interval. Fig. 5 represents a zoom of the variation of the control components during the beginning of the task. As can be seen, the second control component saturate for a while. As the bounds on the actuators dynamics have been considered in the control design, the stability of the closed-loop system is ensured despite of saturations.

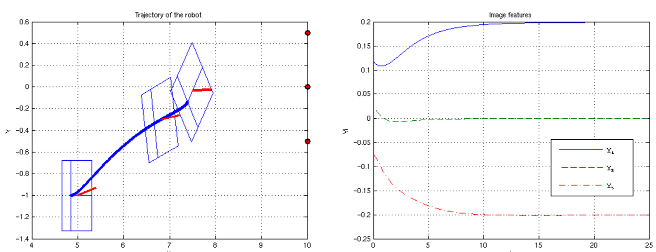

Fig. 3. Trajectory of the robot (left) and visual features (right)

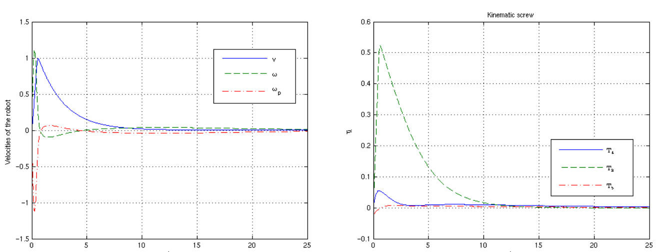

Fig. 4. Robot velocities (left), and camera kinematic screw T (right)

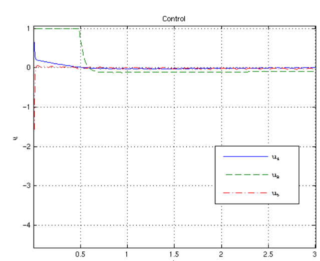

Fig. 5. Control evolution (during the beginning of the task)

V. Concluding Remarks

The works presented in this paper describes an application of advanced control techniques to the design of a multicriteria image-based servoing scheme. The proposed approach allows to consider various kind of constraints at the control synthesis level. By using a representation of the closed-loop system, based of a mixed polytopic and norm-bounded representation of uncertainties with an original sector condition, it was possible to express the different constraints in an LMI form. Following the same reasoning it could be possible to consider bounded uncertainties on the camera intrinsic parameters by introducing additional matrix inequalities. We are currently working on the extension of this control design to consider the case of moving targets.

VI. Acknowledgments

This work was partially conducted within the project EGO-CENTRE supported by the French Interdisciplinary Program in Robotics of CNRS.

References

[1] D. Bellot and P. Danès, “Handling visual servoing schemes through rational systems and LMIs,” IEEE Int. Conference on Decision and Control, Orlando, Florida, December 2001.
[2] F. Chaumette, “Potential problems of stability and convergence in image-based and position-based visual servoing,” in, The confluence of vision and control, D. Kriegman, G. Hager and A. Morse Eds. Berlin, Germany, Springer Verlag, LNCIS Series, Vol. 237, pp. 66-78, 1998.
[3] B. Espiau, F. Chaumette, P. Rives, “A new approach to visual servoing in robotics,” IEEE Transaction on Robotics and Automation, Vol. 8, No 3, June 1992.
[4] J.M. Gomes da Silva Jr. and S. Tarbouriech. “Anti-windup design with guaranteed regions of stability: an LMI-based approach,” IEEE Trans. Autom. Control, vol.50, no.1, pp.106-111, 2005.
[5] K. Hashimoto and T. Noritsugu, “Enlargement of stable region in visual servo,” IEEE Int. Conf. on Decision and Control, Sydney, Australia, December 2000.
[6] S. Hutchinson, G.D. Hager, and P.I. Corke, “A tutorial on visual servo control,” IEEE Transactions on Robotics and Automation, Vol. 12, 5, pp. 651-670, 1996
[7] R. Kelly, “Robust Asymptotic Stable Visual Servoing of Planar Robots,” IEEE Trans. on Robotics and Automation, Vol. 15, 2, pp. 759-766, 1996.
[8] E. Malis and F. Chaumette, “Theoretical Improvement in the Syability Analysis of a New Class of Model-Free Visual Servoing Methods,” IEEE Trans. on Robotics and Automation, Vol. 18, 2, April 2002.
[9] E. Malis and P. Rives, “Robustness of Image-based Visual servoing with respect to Depth Distribution Errors,” IEEE Int. Conf. on Robotics and Automation, Taipei, Taiwan, September 2003.
[10] E. Marchand, A. Comport, F. Chaumette, “Improvements in robust 2D visual servoing,” IEEE Int. Conf. on Robotics and Automation, New Orleans, LA, April 2004.
[11] Y. Mezouar and F. Chaumette, “Path planning for robust image-based control,” IEEE Trans. On Robotics and Automation, vol. 18, 4, pp. 534-549, August 2002.
[12] C. Samson, M. Le Borgne, B. Espiau, “Robot Control, The task function approach,” Oxford Sciences Publications, 1991.
[13] F. Schramm, G. Morel, A. Micaelli, A. Lottin, “Extended-2D Visual Servoing,” IEEE Int. Conf. on Robotics and Automation, New Orleans, LA, April 2004.
[14] M. Sznaier, B. Murphy, O.J. Camps, “An LPV approach to synthesizing robust active vision,” IEEE Int. Conf. on Decision and Control, Sydney, Australia, December 2000.
[15] B. Thuilot, P. Martinet, L. Cordesses, J. Gallice, “Position based visual servoing: keeping the object in the field of vision,” IEEE Int. Conf. on Robotics and Automation, Washington DC, May 2002.
[16] S. Tarbouriech, C. Prieur, J.M. Gomes da Silva Jr., “Stability analysis and stabilization of systems presenting nested saturations,” 43nd IEEE Conference on Decision and Control, Atlantis, Paradise Island (Bahamas), December 2004.
[17] S. Tarbouriech and P. Souères, “Advanced control strategies for the visual servoing scheme,” IFAC Int. Symposium on Robot Control, Karlsruhe, Germany, September 2000.
[18] C.J. Taylor and J.P. Ostrowski, “Robust vision-based control,” IEEE Int. Conf. on Robotics and Automation, San Fransisco, CA, April 2000.
[19] P. Zanne, G. Morel and F. Plestan, “Robust 3D Vision Based Control and Planning,” IEEE Int. Conf. on Robotics and Automation, New Orleans, LA, April 2004.